nature geoscience

Article

https://doi.org/10.1038/s41561-023-01247-7

Recent trends in the chemistry of major northern rivers signal widespread Arctic change

Received: 30 January 2023

Accepted: 10 July 2023

Published online: 21 August 2023

Check for updates

Suzanne E. Tank[1] ✉, James W. McClelland[2], Robert G. M. Spencer[3], Alexander I. Shiklomanov[4], Anya Suslova[5], Florentina Moatar[6], Rainer M. W. Amon[7,8], Lee W. Cooper[9], Greg Elias[10], Vyacheslav V. Gordeev[11], Christopher Guay[12], Tatiana Yu. Gurtovaya[13], Lyudmila S. Kosmenko[14], Edda A. Mutter[15], Bruce J. Peterson[2], Bernhard Peucker-Ehrenbrink[16], Peter A. Raymond[17], Paul F. Schuster[18], Lindsay Scott[5], Robin Staples[19], Robert G. Striegl[18], Mikhail Tretiakov[20], Alexander V. Zhulidov[13], Nikita Zimov[21], Sergey Zimov[21] & Robert M. Holmes[5]

Rivers integrate processes occurring throughout their watersheds and are therefore sentinels of change across broad spatial scales. River chemistry also regulates ecosystem function across Earth's land–ocean continuum, exerting control from the micro- (for example, local food web) to the macro- (for example, global carbon cycle) scale. In the rapidly warming Arctic, a wide range of processes—from permafrost thaw to biological uptake and transformation—might reasonably alter river water chemistry. Here we use data from major rivers that collectively drain two-thirds of the Arctic Ocean watershed to assess widespread change in biogeochemical function within the pan-Arctic basin from 2003 to 2019. While the oceanward flux of alkalinity and associated ions increased markedly over this time frame, nitrate and other inorganic nutrient fluxes declined. Fluxes of dissolved organic carbon showed no overall trend. This divergence in response indicates the perturbation of multiple processes on land, with implications for biogeochemical cycling in the coastal ocean. We anticipate that these findings will facilitate refinement of conceptual and numerical models of current and future functioning of Arctic coastal ecosystems and spur research on scale-dependent change across the river-integrated Arctic domain.

Large rivers are planetary linchpins, connecting vast swaths of terrestrial landmass to the world's coastal oceans. On land, rivers integrate patchy landscapes and the variable biogeochemical processes that these landscapes host, as water moving through watersheds incorporates the chemical signature of its flow path. In the coastal ocean, the chemical signature of water transported by rivers influences nearshore biogeochemical[1,2] and ecological[3,4] function; over broader scales, river water and its composition modify ocean physics[1,5]. Nowhere is this more consequential than in the Arctic, where ~ 11% of Earth's riverine discharge drains into an enclosed basin containing ~ 1% of global ocean volume[6]. This drainage occurs predominantly via six large rivers (Fig. 1 and Extended Data Table 1). As a result, quantifying trends in riverine chemistry at a constrained series of downstream sites allows us to diagnose change across much of the pan-Arctic watershed, better

A full list of affiliations appears at the end of the paper. ✉e-mail: suzanne.tank@ualberta.ca

https://doi.org/10.1038/s41561-023-01247-7

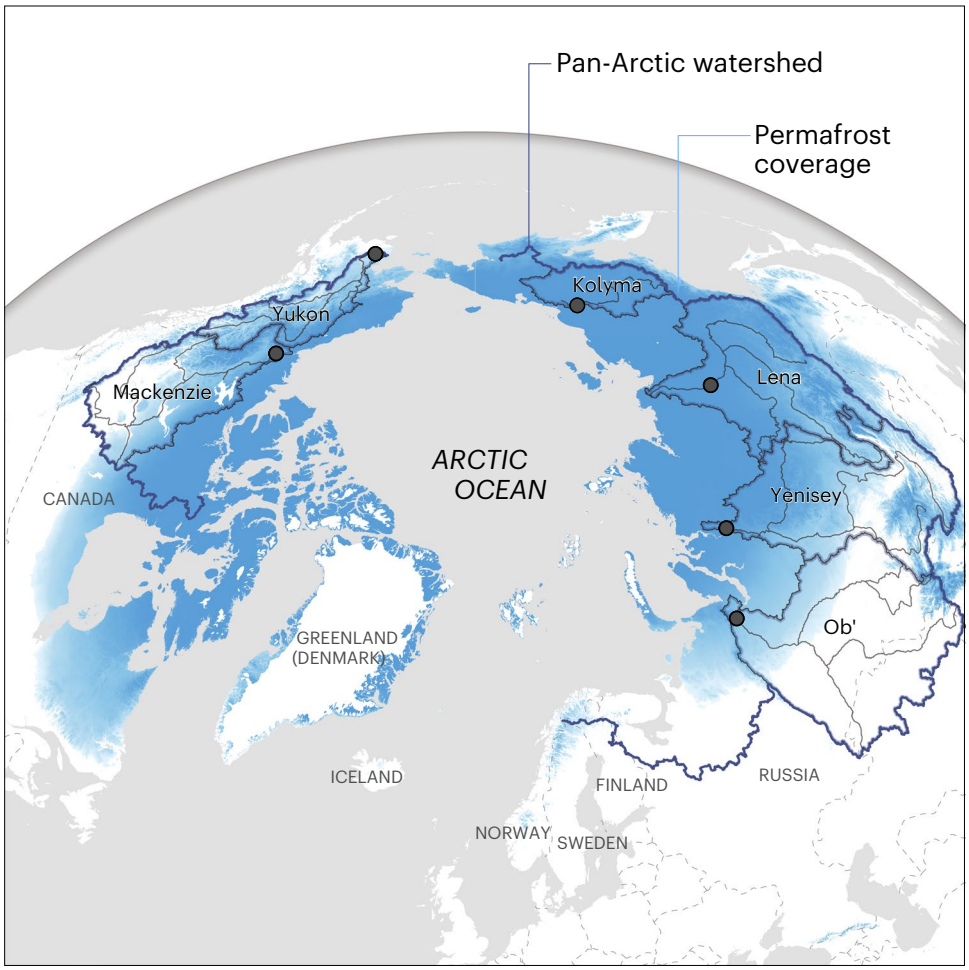

Fig. 1 | The six great Arctic rivers. Sampling locations are indicated by black dots. The 16.8×10^6 km^2 pan-Arctic watershed is delineated by the thick blue line. The northern permafrost extent is indicated using blue shading. Data from Gruber[59], Natural Earth Data and Esri. Credit: Greg Fiske.

understand the current functioning of the connected land–ocean Arctic system and predict what the future may hold for this rapidly changing region[7].

Past research on northern rivers has established significant increases in discharge across the pan-Arctic since the early-mid twentieth century[8,9], attributed to intensification of the hydrologic cycle[10]. Such increases in water transport suggest that we should expect long-term change in the riverine flux (that is, total riverine transport, as mass per time) of biogeochemical constituents, particularly for constituents such as organic carbon that are transport-limited rather than supply-limited in the North[11,12]. Similarly, there is a broadly articulated expectation that permafrost thaw will increase the transport of organic matter, nutrients and ions to aquatic networks, and thus their delivery to the coastal ocean[13–15]. However, change in the North is multi-faceted[16], with processes such as shrubification[17]; temperature-induced increases in biogeochemical processing rates by heterotrophic and autotrophic microbes[18–20]; disturbances such as wildfire[21]; and human modifications such as river impoundment[22–24], changing land use[25] and changing deposition of elements such as N and S[26] often occurring simultaneously. Even for permafrost thaw, the mode of thaw (thermokarst or active layer deepening) and composition of regional soils will shape the biogeochemical response[27]. Rivers integrate all of these processes, providing a signal that reflects the culmination of their effects. Thus, in the face of multi-faceted global change, we should expect the integrated signature of river water to provide a net response that ranges from antagonistic (dampened) to additive[28], depending on the cohesion in directionality of individual effects. Given the nested nature of fluvial networks, the response to change may also be scale dependent, varying with catchment size, transit downstream and the residence time of catchment–water interactions[27].

Here we examine a nearly 20-year record of coupled river discharge and chemistry (Extended Data Fig. 1) collected from the six largest rivers that drain to the Arctic Ocean. These rivers—the Ob', Yenisey, Lena and Kolyma in Russia, and the Mackenzie and Yukon in North America—capture two-thirds of the Arctic Ocean watershed area (Fig. 1 and Extended Data Table 1). Coordinated efforts to collect chemistry data for these rivers started in 2003, whereas discharge records extend much further back in time (Fig. 2). The chemistry data record is the result of our group's ongoing efforts via the Arctic Great Rivers Observatory (ArcticGRO; www.arcticgreatrivers.org), which—given the challenge of collecting methodologically consistent and seasonally representative samples across these diverse jurisdictions and sites—represents an unparalleled resource for exploring Arctic riverine change. Our analyses reveal trends at magnitudes that signal broad-scale perturbation throughout the pan-Arctic but with divergent trajectories that shed light on variable mechanisms of change. We use these insights to consider potential drivers of effect and the consequences of observed change, and to explore where knowledge gaps are hampering our ability to understand current and future functioning of the land–ocean Arctic system.

https://doi.org/10.1038/s41561-023-01247-7

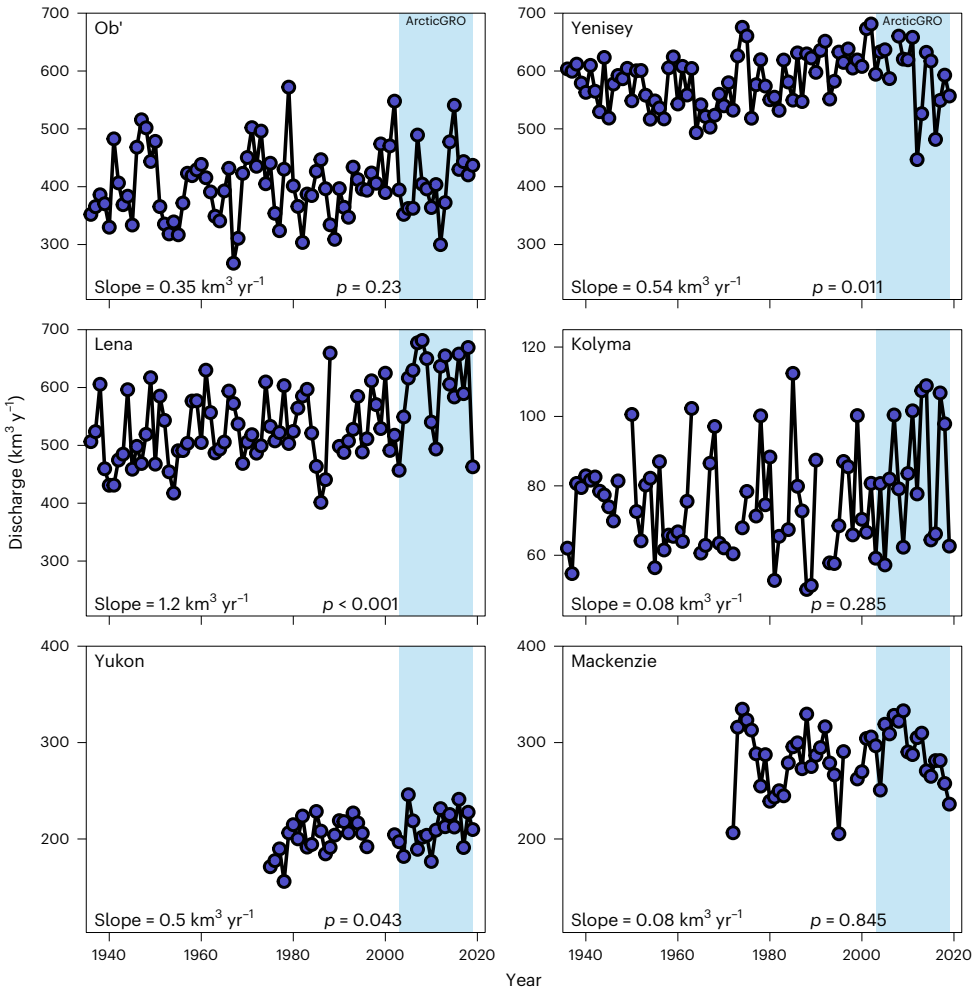

Fig. 2 | Long-term discharge record for each of the six great Arctic rivers. Plots show the full data record for individual rivers, as measured by relevant federal agencies. The time span of the ArcticGRO data record is indicated with blue shading. Trend analyses for the ArcticGRO period of record are provided in Fig. 4b.

Pronounced but divergent trends in Arctic riverine flux

We focus our assessment on three chemical constituents that are important drivers of biogeochemical function across the land–ocean Arctic domain and that are also representative of broader constituent classes. These are: dissolved organic carbon (DOC; representative of the broader organic matter pool including organic-associated nutrients); alkalinity (representative of many dissolved ions) and nitrate (NO_3^-; representative of dissolved inorganic nutrients, including ammonium (NH_4^+) and silica (SiO_2)) (relationships between constituents in Extended Data Fig. 2). To assess constituent flux (the product of concentration and discharge), we applied a modelling approach that couples daily discharge data with more sporadic concentration measurements and develops a relationship between concentration and discharge that is then used to interpolate to dates where discharge data, but not concentration, are available (Methods)[29]. Of our focal suite, only alkalinity experienced a pan-Arctic (that is, six rivers combined) increase in annual flux over our period of record (Fig. 3a). Nitrate declined significantly, while DOC, which has often been a focus of study given its role as a rapid-cycling component of the contemporary carbon cycle, showed no discernable change at the pan-Arctic scale (Fig. 3b,c). Change that did occur, however, was substantial, with a 32% decline in NO_3^- and an 18% increase in alkalinity over a period of 17 years. An assessment of trends in flux across the broad suite of constituents measured by the ArcticGRO programme (Extended Data Fig. 3) reveals patterns within-constituent classes (that is, Extended Data Fig. 2) that generally track those for the focal constituents. For example, trends in flux for ions closely affiliated with alkalinity (Ca^{2+}, Mg^{2+}, Li^+, Sr^{2+}) largely tracked that constituent; inorganic nutrients (SiO_2 and NH_4^+) showed a pan-Arctic decline similar to that for NO_3^-; and patterns for organic-associated nutrients (total dissolved phosphorus) were similar to those for DOC. Given that these constituents are regulated by processes ranging from chemical weathering[30] to biological uptake[18–20] on land and modify processes ranging from ocean acidification[31] to primary production[32] in the coastal ocean, the ecological and biogeochemical ramifications of the changes we observe are likely profound.

Concentration and discharge direct changing flux

In some cases, river-specific trends in constituent flux deviated from the pan-Arctic sum. For example, NO_3^- increased modestly in the Yukon ($p = 0.12$) and showed little change in the Ob' ($p = 0.70$) despite the pan-Arctic decline described above; alkalinity patterns for the Mackenzie (negative trend slope; $p = 0.54$) contrasted with clear increases elsewhere; and DOC increased in the Ob' and decreased in the Yenisey ($p < 0.02$) in the face of limited change in other rivers ($p = 0.23$–0.84); (Fig. 4a). In part, these patterns appeared to be driven by river-specific trends in discharge, which decreased in the Mackenzie ($p = 0.02$) and Yenisey ($p = 0.09$) over the 17-year length of our data record (Fig. 4b) despite the longer-term increase in discharge established

https://doi.org/10.1038/s41561-023-01247-7

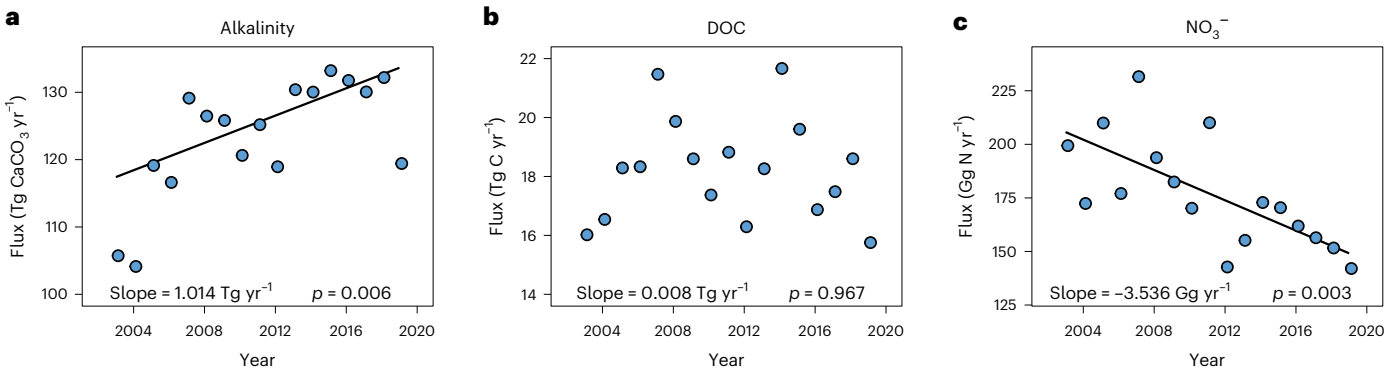

Fig. 3 | Annual constituent flux for alkalinity, DOC and nitrate (NO_3^--N), summed across the six great Arctic rivers. Thiel–Sen slopes with $p < 0.05$ are indicated as lines within each panel. Trends for individual rivers are provided in Fig. 4a.

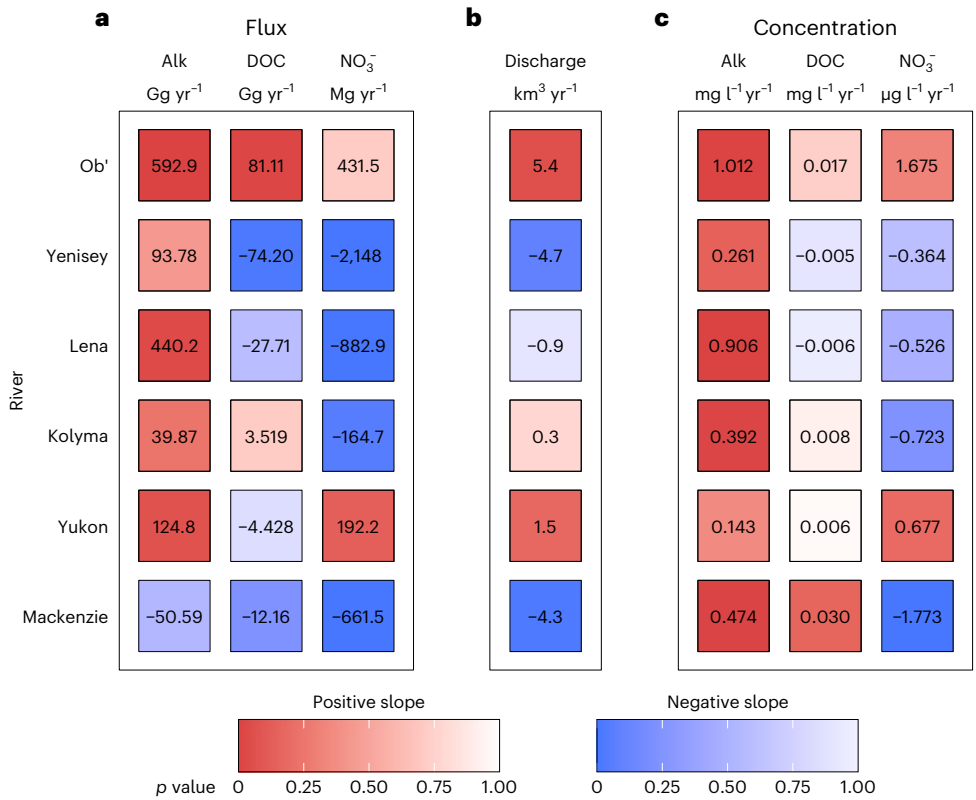

Fig. 4 | Annual trends for each of the six great Arctic rivers. Panels **a**–**c** show constituent flux (**a**), discharge (**b**) and concentration (**c**), focused on the three focal constituents. In each panel, the Sen's slope (numerical value) and *p* value of the trend (shading) are shown. Flux and concentration trends for the full ArcticGRO constituent list are shown in Extended Data Figs. 3 and 4, respectively; detailed statistical outputs are provided in Supplementary Tables 1 and 2. For each panel, the trend analysis covers the 2003–2019 ArcticGRO period.

for the pan-Arctic domain[8,9]. Examining the mechanisms underlying these changes in constituent flux requires that we disentangle inter-annual and long-term change in water discharge from co-occurring trends in concentration. This task is complicated by the fact that constituent concentrations vary seasonally and with discharge itself. We use two distinct approaches to resolve these two known concerns.

First, we use an approach to directly examine trends in measured concentrations, via trend analyses that are binned by season to account for seasonal variation in concentration unrelated to directional change over time (Methods). We target this approach specifically to account for changes to the within-year seasonality of sampling across the two-decade time span of the ArcticGRO programme. Results from this direct trend analysis for concentration (Fig. 4c and Extended Data Fig. 4) are generally similar to those for flux, described above (Fig. 4a and Extended Data Fig. 3). Increases in alkalinity are widespread ($p = 0.00$–0.14 in all rivers except the Yukon), NO_3^- concentrations decline across most rivers and trends for DOC concentration are largely absent ($p = 0.73$–0.96) in all rivers except for the Mackenzie, where DOC concentration increases modestly over time ($p = 0.16$).

Second, we assess changes in flux controlled for inter-annual variation in discharge via a flow-normalization modelling approach that removes variation in discharge across years but retains within-year (that is, day-to-day) seasonality. Although this method does not generate an estimate of 'true' flux as provided in the section

https://doi.org/10.1038/s41561-023-01247-7

above (Figs. 3 and 4a), it is preferred when the analytical emphasis is mechanistic in nature (Methods)[33] because it overcomes year-to-year fluctuations in discharge that can obscure underlying change. These flow-normalized fluxes (Extended Data Fig. 5) show trends that largely reflect those for concentration presented above (Fig. 4c) with some notable refinements: increases in alkalinity and decreases in NO_3^- become more robust, and a decrease in DOC emerges for the Kolyma while the DOC increase in the Mackenzie is maintained. Overall, patterns for flow-normalized fluxes are remarkably similar to those for the best estimates of true flux and concentration presented above, with broad-scale increases in alkalinity and declines in NO_3^- and variable and modest trends for DOC. Taken together, these broad but divergent trends diagnose a multi-system perturbation within the pan-Arctic domain, with effects profound enough to reach the mouths of large northern rivers.

Divergent trends diagnose multi-system change

The array of factors that might reasonably enable long-term change in riverine chemistry is diverse, varying regionally in magnitude and across chemical constituents in effect (Fig. 5 and Supplementary Discussion). As just one example, permafrost thaw via thermokarst (that is, landscape collapse) is a regionally specific phenomena dependent on the presence of ground ice[34] that is generally understood to increase the transport of some constituents to riverine networks (for example, inorganic nutrients)[27] but potentially decrease others (for example, DOC, in cases where landscape collapse promotes mineral sorption or diverts hydrologic flow paths through mineral soils)[35,36]. As a result, the variation in response that we describe above can be used to diagnose drivers of change and develop approaches to assess future functioning of the land–ocean Arctic system. Here we consider a suite of well-documented factors of northern biogeochemical change and the effect of within-constituent cohesion or antagonism on the overall biogeochemical response. An expansion of this assessment is provided in the Supplementary Discussion.

For some chemical constituents, known factors of change are both relatively widespread and consistent in their directionality (Fig. 5). In the case of alkalinity and associated ions (Extended Data Fig. 2), for example, exposure to deeper soils via either active layer deepening or thermokarst-associated permafrost thaw will typically increase mineral weathering by increasing water contact with deeper mineral soils[37,38]. Acting additively, shrubification[39] and increased temperature-driven organic matter processing[40] will increase weathering rates via processes such as increasing soil pore water acidity. Because these processes are coherent in their directionality and geographically widespread, the net result appears as a cohesive increase in alkalinity concentration and flux throughout the pan-Arctic domain.

For other constituents, variation in the directionality of factors of change appears to cause a muted overall response. In the case of DOC, for example, permafrost thaw can either increase[41] or decrease[35] loading to aquatic systems, depending on the composition of soils subject to thaw[36]. While shrubification will increase vegetation and litter substrates for leaching and therefore the transport of organic matter to aquatic networks[42], temperature-driven increases in mineralization[20,43] and potential rapid processing of novel organic matter substrates[44] act in opposition to this effect. Across these large Arctic rivers, the result appears to be a dissipation of effect with transport through aquatic networks, with factors of change that act antagonistically and enable little net change in DOC delivery to the coastal ocean over the time span of this assessment.

Finally, in some cases, geographically widespread processes appear to overwhelm counteracting drivers. For example, although we broadly expect permafrost thaw to increase inorganic nitrogen delivery to aquatic networks[27], our analyses reveal declines in the transport of NO_3^- (and associated inorganic nutrients; Extended Data Figs. 2 and 3) to the Arctic Ocean from large Arctic rivers. This suggests that factors

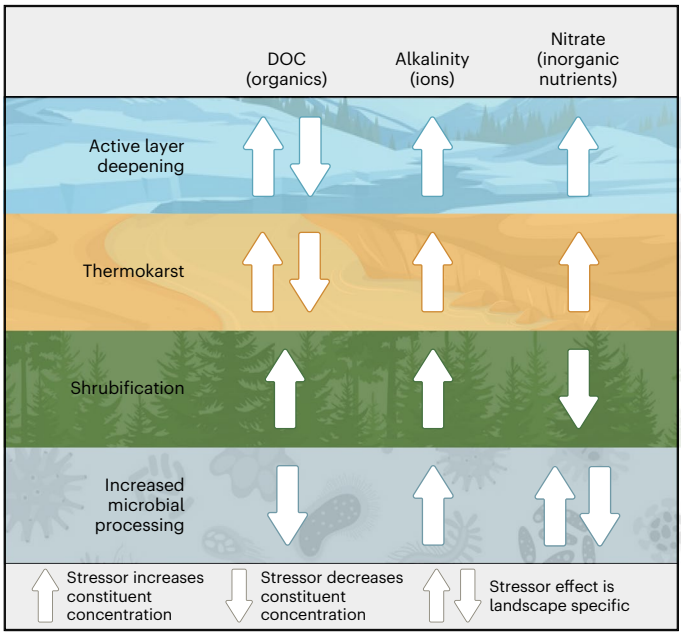

Fig. 5 | A conceptual diagram illustrating select drivers of change of Arctic riverine chemistry. Arrows indicate anticipated direction of effect for each of the three focal constituents. The Supplementary Discussion provides a detailed overview of literature evidence for this conceptual exercise, in addition to a description of several drivers (acid deposition, impoundment, land use and land cover change, wildfire) that are not included in this conceptual illustration. Credit: Julianne Waite.

such as temperature-driven increases in nitrogen cycling[19] or nitrogen uptake and/or immobilization[18,45] may be overwhelming local increases in mobilization[27] when assessed at the large-river watershed scale. These findings underline the importance of taking a systems approach to understanding Arctic change, with an acknowledgement that biogeochemical cycles are inherently linked across elements and space.

Broad perturbation across the land–ocean Arctic domain

Our analyses diagnose pervasive changes to the land–ocean Arctic system, signalling domain-scale alteration to biogeochemical and ecosystem function. On land, ecosystem models have predicted increases in organic matter loading to fluvial networks in the changing North[16]. The lack of this signal at river outflows, therefore, suggests possible increases in carbon mineralization and associated outgassing during transit through watersheds and thus an acceleration in carbon cycling within Arctic catchments. Increasing alkalinity is suggestive of increases in chemical weathering. In the pan-Arctic, however, a predominance of carbonate over silicate weathering, coupled with substantial sulfide oxidation in some watersheds, causes the ratio of CO_2 consumption:alkalinity generation to be overall low relative to the global mean[30]. As a result, increasing SO_4^{2-} fluxes (Extended Data Fig. 3) in a region where SO_4^{2-} may be largely derived from sulfides (documented for Yukon, Kolyma, Mackenzie[46]) may in fact indicate increasing bicarbonate liberation in the absence of CO_2 fixation[30].

In the coastal ocean, riverine inputs of dissolved inorganic carbon result in CO_2 outgassing to the atmosphere[47]. The magnitude of this effect relative to weathering-induced CO_2 fixation on land, and its change, will play a key role in determining the carbon balance of the Arctic system. Acting concurrently, the declining NO_3^- that we document is consistent with negative feedbacks for Arctic Ocean biological productivity and CO_2 uptake from the atmosphere, which is generally thought to be increasing as seasonal sea ice declines and nutrients

become more available[48]. However, the Arctic Ocean also has globally low N:P ratios because its shelf sediments are a substantial nitrogen sink through denitrification[49]. As a result, decreases in riverine NO_3^- transport coupled with increasing discharge will strengthen stratification and decrease availability of nutrients for biological production. These changes will play out alongside other co-occurring processes, such as changes to the dilution effect of river water on ocean pH[30] with increasing alkalinity, which may also affect biological function[50].

Emergent priorities and considerations of scale

In addition to implications for the current and future functioning of the Arctic system, our findings point to several important pathways forward for understanding land–ocean Arctic change. We highlight several of these here. First, particularly for bio-reactive constituents (DOC, nutrients), this work illustrates the importance of scale. Widespread declines in constituents such as NO_3^- in the face of local processes known to increase land–water mobilization suggest a possible redistribution in biogeochemical processing at the landscape scale, where local increases in biological uptake and transformation are decreasing the transport of bio-reactive constituents downstream. How the balance between local mobilization and broad-scale processing may shift for the smaller catchments encircling the Arctic Ocean (for example, NO_3^- trends in refs. 51,52), which are characterized by shorter in-river residence times and different vegetation cover and soil characteristics[53,54], remains an open question. Determining oceanward flux in smaller, more northerly catchments is thus a clear priority[55]. Nested studies to assess how Arctic system change alters the propagation of biogeochemical constituents through fluvial networks will also be helpful on this front. Second, teasing apart the relative importance of various drivers of change, and how these will vary with time and across constituents, will require investment in process-based models, as already developed for alkalinity[40] and DOC[16], in addition to models that are linked across elements and space[47]. These models must inherently co-consider multiple drivers of change, including those not directly addressed here (broader assessment of drivers is in the Supplementary Discussion). An exploration of the effects of changing seasonality, such as offsets between the temperature-driven expansion of the thaw season relative to light-driven constraints on primary production, might also be better resolved in this context[56,57]. Third, while discharge records on large Arctic rivers began as early as the 1930s (Fig. 2), the cohesive biogeochemical sampling reported here was initiated in 2003. Given the known effect of discharge on biogeochemical concentration in large Arctic rivers[11,58], models that consider the effects of longer-term change in discharge on biogeochemical flux are a priority, particularly given the strong trends documented for northern discharge at the end of the twentieth century[8].

While the datasets we draw on for our analyses are remarkable for their geographic cohesion and their relative length, they also diagnose profound, rapid change. Our results clearly call for continued, integrated observation of the land–ocean Arctic system across all jurisdictions that constitute the pan-Arctic domain. Just as importantly, however, they reinforce the need for rapid attention to Earth's warming climate and its multiplicative effects in the North.

Online content

Any methods, additional references, Nature Portfolio reporting summaries, source data, extended data, supplementary information, acknowledgements, peer review information; details of author contributions and competing interests; and statements of data and code availability are available at https://doi.org/10.1038/s41561-023-01247-7.

References

1. Carmack, E. C. et al. Freshwater and its role in the Arctic marine system: sources, disposition, storage, export, and physical and biogeochemical consequences in the Arctic and global oceans. *J. Geophys. Res. Biogeosci.* **121**, 675–717 (2016).
2. Dai, M. et al. Carbon fluxes in the coastal ocean: synthesis, boundary processes, and future trends. *Annu. Rev. Earth Planet. Sci.* **50**, 593–626 (2022).
3. Dunton, K. H., Weingartner, T. & Carmack, E. C. The nearshore western Beaufort Sea ecosystem: circulation and importance of terrestrial carbon in arctic coastal food webs. *Prog. Oceanogr.* **71**, 362–378 (2006).
4. Lacroix, F., Ilyina, T., Mathis, M., Laruelle, G. G. & Regnier, P. Historical increases in land-derived nutrient inputs may alleviate effects of a changing physical climate on the oceanic carbon cycle. *Glob. Change Biol.* **27**, 5491–5513 (2021).
5. Liu, X. et al. Simulating water residence time in the coastal ocean: a global perspective. *Geophys. Res. Lett.* **46**, 13910–13919 (2019).
6. McClelland, J. W., Holmes, R. M., Dunton, K. H. & Macdonald, R. W. The Arctic Ocean estuary. *Estuaries Coasts* **35**, 353–368 (2012).
7. Previdi, M., Smith, K. L. & Polvani, L. M. Arctic amplification of climate change: a review of underlying mechanisms. *Environ. Res. Lett.* **16**, 093003 (2021).
8. Peterson, B. J. et al. Increasing river discharge to the arctic ocean. *Science* **298**, 2171–2173 (2002).
9. Ahmed, R., Prowse, T., Dibike, Y., Bonsal, B. & O'Neil, H. Recent trends in freshwater influx to the Arctic Ocean from four major Arctic-draining rivers. *Water* **12**, 1189 (2020).
10. Rawlins, M. A. et al. Analysis of the Arctic system for freshwater cycle intensification: observations and expectations. *J. Clim.* **23**, 5715–5737 (2010).
11. Raymond, P. A. et al. Flux and age of dissolved organic carbon exported to the Arctic Ocean: a carbon isotopic study of the five largest arctic rivers. *Glob. Biogeochem. Cycles* **21**, GB4011 (2007).
12. Gómez-Gener, L., Hotchkiss, E. R., Laudon, H. & Sponseller, R. A. Integrating discharge-concentration dynamics across carbon forms in a boreal landscape. *Water Resour. Res.* **57**, e2020WR028806 (2021).
13. Toohey, R. C., Herman-Mercer, N. M., Schuster, P. F., Mutter, E. A. & Koch, J. C. Multidecadal increases in the Yukon River Basin of chemical fluxes as indicators of changing flowpaths, groundwater, and permafrost. *Geophys. Res. Lett.* **43**, 12,120–112,130 (2016).
14. Shogren, A. J. et al. Revealing biogeochemical signatures of Arctic landscapes with river chemistry. *Sci. Rep.* **9**, 12894 (2019).
15. Gabysheva, O. I., Gabyshev, V. A. & Barinova, S. Influence of the active layer thickness of permafrost in eastern Siberia on the river discharge of nutrients into the Arctic Ocean. *Water* **14**, 84 (2022).
16. Kicklighter, D. W. et al. Insights and issues with simulating terrestrial DOC loading of Arctic river networks. *Ecol. Appl.* **23**, 1817–1836 (2013).
17. Tape, K., Sturm, M. & Racine, C. The evidence for shrub expansion in Northern Alaska and the Pan-Arctic. *Glob. Change Biol.* **12**, 686–702 (2006).
18. Reay, D. S., Nedwell, D. B., Priddle, J. & Ellis-Evans, J. C. Temperature dependence of inorganic nitrogen uptake: reduced affinity for nitrate at suboptimal temperatures in both algae and bacteria. *Appl. Environ. Microb.* **65**, 2577–2584 (1999).
19. Salazar, A., Rousk, K., Jónsdóttir, I. S., Bellenger, J.-P. & Andrésson, Ó. S. Faster nitrogen cycling and more fungal and root biomass in cold ecosystems under experimental warming: a meta-analysis. *Ecology* **101**, e02938 (2020).
20. Wickland, K. P. et al. Biodegradability of dissolved organic carbon in the Yukon River and its tributaries: seasonality and importance of inorganic nitrogen. *Glob. Biogeochem. Cycles* **26**, GB0E03 (2012).
21. Box, J. E. et al. Key indicators of Arctic climate change: 1971–2017. *Environ. Res. Lett.* **14**, 045010 (2019).
22. Maavara, T. et al. River dam impacts on biogeochemical cycling. *Nat. Rev. Earth Environ.* **1**, 103–116 (2020).

23. Zolkos, S. et al. Multidecadal declines in particulate mercury and sediment export from Russian rivers in the pan-Arctic basin. *Proc. Natl. Acad. Sci. USA* **119**, e2119857119 (2022).
24. Shiklomanov, A. et al. in *Arctic Hydrology, Permafrost and Ecosystems* (eds Yang, D. & Kane, D. L.) 703–738 (Springer International Publishing, 2021).
25. Bergen, K. M. et al. Long-term trends in anthropogenic land use in Siberia and the Russian Far East: a case study synthesis from Landsat. *Environ. Res. Lett.* **15**, 105007 (2020).
26. Aas, W. et al. Global and regional trends of atmospheric sulfur. *Sci. Rep.* **9**, 953 (2019).
27. Tank, S. E. et al. Landscape matters: predicting the biogeochemical effects of permafrost thaw on aquatic networks with a state factor approach. *Permafrost Periglacial Processes* **31**, 358–370 (2020).
28. Slaveykova, V. I. Biogeochemical dynamics research in the Anthropocene. *Front. Environ. Sci.* https://doi.org/10.3389/fenvs.2019.00090 (2019).
29. Hirsch, R. M., Moyer, D. L. & Archfield, S. A. Weighted regressions on time, discharge, and season (WRTDS), with an application to Chesapeake Bay River inputs. *JAWRA J. Am. Water Resour. Assoc.* **46**, 857–880 (2010).
30. Tank, S. E. et al. A land-to-ocean perspective on the magnitude, source and implication of DIC flux from major Arctic rivers to the Arctic Ocean. *Glob. Biogeochem. Cycles* **26**, GB4018 (2012).
31. Terhaar, J., Orr, J. C., Ethé, C., Regnier, P. & Bopp, L. Simulated Arctic Ocean response to doubling of riverine carbon and nutrient delivery. *Glob. Biogeochem. Cycles* **33**, 1048–1070 (2019).
32. Terhaar, J., Lauerwald, R., Regnier, P., Gruber, N. & Bopp, L. Around one third of current Arctic Ocean primary production sustained by rivers and coastal erosion. *Nat. Commun.* **12**, 169 (2021).
33. Hirsch, R. M., Archfield, S. A. & De Cicco, L. A. A bootstrap method for estimating uncertainty of water quality trends. *Environ. Modell. Software* **73**, 148–166 (2015).
34. Kokelj, S. V. & Jorgenson, M. T. Advances in thermokarst research. *Permafrost Periglacial Processes* **24**, 108–119 (2013).
35. Littlefair, C. A., Tank, S. E. & Kokelj, S. V. Retrogressive thaw slumps temper dissolved organic carbon delivery to streams of the Peel Plateau, NWT, Canada. *Biogeosciences* **14**, 5487–5505 (2017).
36. Frey, K. E. & McClelland, J. W. Impacts of permafrost degradation on Arctic river biogeochemistry. *Hydrol. Processes* **23**, 169–182 (2009).
37. Keller, K., Blum, J. D. & Kling, G. W. Stream geochemistry as an indicator of increasing permafrost thaw depth in an arctic watershed. *Chem. Geol.* **273**, 76–81 (2010).
38. Zolkos, S., Tank, S. E. & Kokelj, S. V. Mineral weathering and the permafrost carbon-climate feedback. *Geophys. Res. Lett.* **45**, 9623–9632 (2018).
39. Berner, R. A. The carbon cycle and CO_2 over Phanerozoic time: the role of land plants. *Philos. Trans. R. Soc. B.* **353**, 75–81 (1998).
40. Beaulieu, E., Godderis, Y., Donnadieu, Y., Labat, D. & Roelandt, C. High sensitivity of the continental-weathering carbon dioxide sink to future climate change. *Nat. Clim. Change* **2**, 346–349 (2012).
41. Vonk, J. E. et al. High biolability of ancient permafrost carbon upon thaw. *Geophys. Res. Lett.* **40**, 2689–2693 (2013).
42. Finstad, A. G. et al. From greening to browning: catchment vegetation development and reduced S-deposition promote organic carbon load on decadal time scales in Nordic lakes. *Sci. Rep.* **6**, 31944 (2016).
43. Moore, T. R., Paré, D. & Boutin, R. Production of dissolved organic carbon in Canadian forest soils. *Ecosystems* **11**, 740–751 (2008).
44. Drake, T. W. et al. The ephemeral signature of permafrost carbon in an Arctic fluvial network. *J. Geophys. Res. Biogeosci.* **123**, 1475–1485 (2018).
45. Hicks Pries, C. E., McLaren, J. R., Smith Vaughn, L., Treat, C. & Voigt, C. in *Multi-scale Biogeochemical Processes in Soil Ecosystems: Critical Reactions and Resilience to Climate Change* Ch. 7 (eds Yang, Y. Y. et al.) 157–191 (John Wiley & Sons, 2022).
46. Burke, A. et al. Sulfur isotopes in rivers: insights into global weathering budgets, pyrite oxidation, and the modern sulfur cycle. *Earth Planet. Sc. Lett.* **496**, 168–177 (2018).
47. Lacroix, F., Ilyina, T. & Hartmann, J. Oceanic CO_2 outgassing and biological production hotspots induced by pre-industrial river loads of nutrients and carbon in a global modeling approach. *Biogeosciences* **17**, 55–88 (2020).
48. Lewis, K. M., van Dijken, G. L. & Arrigo, K. R. Changes in phytoplankton concentration now drive increased Arctic Ocean primary production. *Science* **369**, 198–202 (2020).
49. Chang, B. X. & Devol, A. H. Seasonal and spatial patterns of sedimentary denitrification rates in the Chukchi sea. *Deep Sea Res. Part II* **56**, 1339–1350 (2009).
50. Dutkiewicz, S. et al. Impact of ocean acidification on the structure of future phytoplankton communities. *Nat. Clim. Change* **5**, 1002–1006 (2015).
51. McClelland, J. W., Stieglitz, M., Pan, F., Holmes, R. M. & Peterson, B. J. Recent changes in nitrate and dissolved organic carbon export from the upper Kuparuk River, North Slope, Alaska. *J. Geophys. Res. Biogeosci.* **112**, G04S60 (2007).
52. Kendrick, M. R. et al. Linking permafrost thaw to shifting biogeochemistry and food web resources in an arctic river. *Glob. Change Biol.* **24**, 5738–5750 (2018).
53. Speetjens, N. J. et al. The pan-Arctic catchment database (ARCADE). *Earth Syst. Sci. Data* **15**, 541–554 (2023).
54. Palmtag, J. et al. A high spatial resolution soil carbon and nitrogen dataset for the northern permafrost region based on circumpolar land cover upscaling. *Earth Syst. Sci. Data* **14**, 4095–4110 (2022).
55. Brown, K. A. et al. Geochemistry of small canadian Arctic rivers with diverse geological and hydrological settings. *J. Geophys. Res. Biogeosci.* **125**, e2019JG005414 (2020).
56. Treat, C. C., Wollheim, W. M., Varner, R. K. & Bowden, W. B. Longer thaw seasons increase nitrogen availability for leaching during fall in tundra soils. *Environ. Res. Lett.* **11**, 064013 (2016).
57. Lacroix, F. et al. Mismatch of N release from the permafrost and vegetative uptake opens pathways of increasing nitrous oxide emissions in the high Arctic. *Glob. Change Biol.* **28**, 5973–5990 (2022).
58. Holmes, R. M. et al. Seasonal and annual fluxes of nutrients and organic matter from large rivers to the Arctic Ocean and surrounding seas. *Estuaries Coasts* **35**, 369–382 (2012).
59. Gruber, S. Derivation and analysis of a high-resolution estimate of global permafrost zonation. *The Cryosphere* **6**, 221–233 (2012).

[1]Department of Biological Sciences, University of Alberta, Edmonton, Alberta, Canada. [2]Ecosystems Center, Marine Biological Laboratory, Woods Hole, MA, USA. [3]Department of Earth, Ocean and Atmospheric Science, Florida State University, Tallahassee, FL, USA. [4]Earth Systems Research Center, University of New Hampshire, Durham, NH, USA. [5]Woodwell Climate Research Center, Falmouth, MA, USA. [6]INRAE, UR RiverLy, Centre de Lyon-Villeurbanne, France. [7]Department of Marine and Coastal Environmental Sciences, Texas A&M University, Galveston, TX, USA. [8]Department of Oceanography, Texas A&M University, College Station, TX, USA. [9]Chesapeake Biological Laboratory, University of Maryland Center for Environmental Science, Solomons, MD, USA. [10]Western Arctic Research Center, Inuvik, Northwest Territories, Canada. [11]Shirshov Institute of Oceanology, Russian Academy of Sciences, Moscow, Russia. [12]Mamala Research LLC, Honolulu, HI, USA. [13]South Russia Centre for Preparation and Implementation of International Projects, Rostov-on-Don, Russia. [14]Hydrochemical Institute of the Federal Service for Hydrometeorology and Environmental Monitoring, Ministry of Natural Resources and Environment of the Russian Federation, Rostov-on-Don, Russia. [15]Yukon River Inter-Tribal Watershed Council, Anchorage, AK, USA. [16]Marine Chemistry and Geochemistry Department, Woods Hole Oceanographic Institution, Woods Hole, MA, USA. [17]School of Forestry and Environmental Studies, Yale University, New Haven, CT, USA. [18]Earth System Processes Division, US Geological Survey, Boulder, CO, USA. [19]Water Resources Division, Government of the Northwest Territories, Yellowknife, Northwest Territories, Canada. [20]River Estuaries and Water Resources Department, Arctic and Antarctic Research Institute, Saint Petersburg, Russia. [21]Pacific Geographical Institute of the Far Eastern Branch of the Russian Academy of Sciences, Chersky, Russia. ✉e-mail: suzanne.tank@ualberta.ca

Methods

Sample collection and dataset coverage

Water chemistry. We began sampling the six largest Arctic rivers for water chemistry in the summer of 2003. The project was initially called PARTNERS (Pan-Arctic River Transport of Nutrients, Organic Matter and Suspended Sediments) and was expanded and renamed the Arctic Great Rivers Observatory (ArcticGRO) in 2008. Sample collection for the data presented in this study occurred five to seven times per year, with the exception of a short break during 2007–2008 (Extended Data Fig. 1). Water chemistry samples are collected as far downstream on each of the six great Arctic rivers as logistically feasible, at Salekhard (Ob'), Dudinka (Yenisey), Zhigansk (Lena), Cherskiy (Kolyma), Pilot Station (Yukon) and Tsiigehtchic (Mackenzie) (Fig. 1; Extended Data Table 1). Between 2003 and 2011, open-water sampling was conducted using a D-96 sampler[60] equipped with a Teflon nozzle and Teflon sample-collection bag, which enabled depth-integrated and flow-weighted samples. Samples were collected at five roughly equal increments across the river channel and combined in a 14 l Teflon churn, resulting in a single composite sample. Beginning in 2012, open-water sampling was conducted by collecting three near-surface samples on each of the left bank, right bank and mid-points of each river and combining these to form a composite sample. Across the full period of record, wintertime (under ice) samples were collected by drilling a hole at the river's mid-point and collecting a sample from below the ice surface.

Within years, the timing of sample collection has changed slightly over the ArcticGRO period of record. Early collection schemes (2003–2006 and 2009–2011) focused on the spring freshet (three or more samples per year), with further sample coverage through the more broadly spread late summer (period of deepest thaw of the seasonally frozen active layer; one to four samples) and winter (typically one sample) periods. Given the paucity of cross-site comparable data for these rivers at the outset of the ArcticGRO programme, this sampling scheme was designed to maximize coverage during the high flows of the spring, when constituent concentrations are changing rapidly and the majority of constituent flux occurs[58]. In 2012, sampling shifted to become evenly spread across the annual cycle, with samples collected bi-monthly (that is, six samples per year) and months of collection alternating between years. Sample processing (filtering and preservation) occurs within 24 hours of sample collection. As described above for sample collection, processing protocols were identical across all sites. Processed and preserved samples were shipped to Woods Hole, Massachusetts, USA, where they were distributed to specialized laboratories for individual analyses. A complete description of processing and analytical methodologies is available on the ArcticGRO website (www.arcticgreatrivers.org) and archived at the Arctic Data Center[61]. The focal constituents highlighted in this study were analysed as follows: for DOC, on a Shimadzu TOC analyser, following acidification with HCl, sparging and using the three of five injections that resulted in the lowest coefficient of variation; for alkalinity, following acid titration using a Hach digital titrator (2003–2009) and Mettler Toledo model T50M titrator (2010 onwards); for NO_3^- (as $NO_3^- + NO_2^-$) colorimetrically using Lachat Quickchem FIA + 8000 (2003–2011) and Astoria (2012 onwards) autoanalysers.

Discharge. All ArcticGRO discharge measurements are from long-term gauging stations operated by Roshydromet, the US Geological Survey and the Water Survey of Canada. On the Ob', Yukon and Mackenzie rivers, gauging stations are identical to the ArcticGRO sample-collection location. On the Yenisey, Lena and Kolyma rivers, proximate gauging stations were used, at Kyusyur, Igarka and Kolymskoye, respectively. The effect of this modest offset, and methods for correction, has been described elsewhere[58]. Continually updated concentration and discharge datasets are available on the ArcticGRO website. Concentration and discharge data used for this analysis (2003–2019, inclusive) have been archived at the Arctic Data Center as a fixed data package (https://doi.org/10.18739/A2VH5CK43).

Uncertainty associated with discharge measurements in major Arctic rivers varies with season and flow rate, with largest error percentages during winter low-flow conditions and smallest error percentages during intermediate-flow conditions during summer. On an annual basis, errors on discharge estimates are typically less than 10% (ref. 62). On the Yukon River, the US Geological Survey conducts a quality control assessment of daily discharge estimates, with accuracy reported in quality bins[63]. Daily discharge values on the Yukon River at Pilot Station are typically rated as 'fair' (within 15% of the true value) during open water and 'less than fair' on days when values are estimated, which typically occurs under ice and during the spring freshet[64]. On the four Russian rivers included here, mean annual discharge errors have been assessed to range from 4.3 to 7.1%, for an assessment of data from 1955 to 2000 (ref. 62). Although declines in the frequency of direct discharge measurements used to update Russian rating curves have probably increased error in recent years[65], an updated assessment of proportional error on discharge for these sites has not been conducted.

Determination of constituent flux using the WRTDS-Kalman approach

Determining constituent flux requires a modelling approach, because discharge data are typically available at daily (or even more refined) time steps, while concentration measurements are almost always collected much more patchily over time. We used the Weighted Regressions on Time, Discharge and Season (WRTDS) approach to estimate constituent flux over the ArcticGRO period of record, actualized in the *EGRET* (Exploration and Graphics for RivEr Trends)[66] package in the R statistical platform[67]. This approach has been shown to provide more accurate estimates of constituent flux than other common statistical techniques used for flux estimation[68], as a result of the use of weighted regression (below) and the removal of the requirement for homoscedastic residuals for bias correction[69]. Similar to other flux estimation techniques, the predictive equation takes the form of:

$$\ln(c) = \beta_0 + \beta_1 t + \beta_2 \ln(Q) + \beta_3 \sin(2\pi t) + \beta_4 \cos(2\pi t) + \varepsilon \quad (1)$$

where c is concentration, Q is discharge, t is time in decimal years and ε is the unexplained variation, with the sine and cosine functions enabling seasonality within the model[29]. However, unlike most other flux modelling approaches, the coefficients β_0–β_4 are not static but are allowed to vary gradually in Q, t space. This is accomplished via an approach that develops a separate model for each day of the observational record by re-evaluating the relationship between concentration and time, season and discharge, with a weighting that prioritizes samples closest in Q, t space to the day of estimation[69]. For this work, we use the WRTDS-Kalman modification, which further improves upon the above-described technique by using a first-order autoregressive (AR1) model to capture residual autocorrelation[70]. An assessment of measured vs modelled daily outputs via WRTDS-Kalman is provided in Supplementary Fig. 1. Daily WRTDS-Kalman flux outputs have been archived at the Arctic Data Center (https://doi.org/10.18739/A2VH5CK43).

Calculation of flow-normalized flux and assessment of flow-normalized trends

A complication of evaluating trends in flux is that a substantial amount of variation in concentration is caused by year-to-year variation in discharge, which adds considerable noise to the time series. To assess changes in flux with year-to-year variation in discharge removed, we use the WRTDS *flow-normalization* technique, which filters out the influence of inter-annual variation in streamflow. This is accomplished by creating a probability density function of Q for each day of the calendar year and producing flow-normalized concentrations and

fluxes that integrates over this probability density function[33]. In this way, discharge is normalized across calendar years, but intra-annual variation (that is, seasonal variation, at a daily time step) is retained. Given the statistical complexity of this smoothing approach, we estimate uncertainty in change over the flow-normalized time series using a block bootstrap technique implemented in the R package *EGRETci*, which creates a posterior mean estimate ($\hat{\pi}$) of the probability of a trend and assesses trend likelihood as: highly likely ($\hat{\pi}$ < 0.05 or >0.95) very likely ($\hat{\pi}$ 0.05–0.10 or 0.90–0.95), likely ($\hat{\pi}$ 0.10–0.33 or 0.66–0.90) or about as likely as not ($\hat{\pi}$ 0.33–0.66)[33]. Our results are provided as mean and 90% confidence interval outputs from the block bootstrap approach described in ref. 33.

Assessment of trends in annual discharge and WRTDS-Kalman constituent flux

Daily discharge and flux estimates were summed within years to generate an annual time series, and a Mann–Kendall test was used to analyse the significance of annual trends over time. Within this analysis, trend slopes were calculated using the Theil–Sen method. Trend analyses and the calculation of slopes were conducted using the *trend* package[71] in R[67]. We report Kendall's *p* value and Sen's slope in the main and Extended Data figures and report additional statistical outputs in Supplementary Table 1. In all cases (that is, including for discharge), our trend analysis spanned the ArcticGRO (2003–2019) analytical window.

Assessment of trends in concentration

To allow us to examine trends in concentration directly but account for seasonal variation in concentration measurements that may skew trend detection, we used a Seasonal Kendall test[72]. This approach accounts for seasonality by calculating the Mann–Kendall statistic for each of *p* seasons directly and then combines the test statistic for each season (S_p) to create an overall seasonal Kendall statistic (S'):

$$S' = \sum_{i=1}^{p} S_p$$

We used a modification of the original Seasonal Kendall test, which accounts for serial dependence by using an autoregressive moving average (1:1) approach[73]. We defined seasons as spring (May–June), summer (July–October) and winter (November–April), as has been previously established for the ArcticGRO dataset[58,74]. We further used a Seasonal Kendall slope estimator to determine the magnitude of trends, following the Theil–Sen approach as modified for the seasonal Kendall test[72]. Results are reported in Extended Data Fig. 4 and Supplementary Table 2.

Ethics and inclusion

This research has been conducted in accordance with the Global Code of Conduct for Research laid out by the TRUST Equitable Research Partnerships. Local researchers have been instrumental throughout the ArcticGRO research process, including during initial project planning; this involvement is reflected in the manuscript's authorship list. Local partners who do not meet *Nature* authorship criteria are listed in the acknowledgements section. Sampling is undertaken in accordance with local permitting requirements, including via the acquisition of a Northwest Territories Scientific Research License for sampling on the Mackenzie River. Results and progress for this ongoing project are communicated via regular interactions with local partners, periodic in-person visits to partner locations in Alaska, Canada and the Russian Federation and broad dissemination of results on the project website (www.arcticgreatrivers.org).

Data visualization

Figures 2–4, Extended Data Figs. 1 and 3–5 and Supplementary Fig. 1 were actualized in R[67] using *ggplot2* (ref. 75). The correlation cluster analysis shown in Extended Data Fig. 2 was carried out using the function 'heatmap.2' in the *gplots* package[76] in R.

Data availability

Data used for our analyses and daily Kalman outputs are provided as a fixed package at the Arctic Data Center (https://doi.org/10.18739/A2VH5CK43). More recent updates of the ArcticGRO water quality and discharge datasets can be found at the project website (www.arcticgreatrivers.org) and through the Arctic Data Center[61].

References

60. Davis, B. E. *A Guide to the Proper Selection and Use of Federally Approved Sediment and Water-Quality Samplers*. Report No. 2005-1087 (United States Geological Survey, 2005).
61. Holmes, R. M., McClelland, J., Tank, S., Spencer, R. & Shiklomanov, A. Arctic Great Rivers Observatory IV biogeochemistry and discharge data: 2020–2024. *Arctic Data Center* https://doi.org/10.18739/A2XW47X7D (2022).
62. Shiklomanov, A. I. et al. Cold region river discharge uncertainty—estimates from large Russian rivers. *J. Hydrol.* **326**, 231–256 (2006).
63. US Geological Survey *Annual Water Data Report Documentation* (USGS, accessed 11 April 2023); https://wdr.water.usgs.gov/current/documentation.html
64. US Geological Survey *Annual Water Data Report, Site 15565447* (USGS, accessed 11 April 2023); https://wdr.water.usgs.gov/index.html
65. Tretiyakov, M. V., Muzhdaba, O. V., Piskun, A. A. & Terekhova, R. A. The state of the Roshydromet Hydrological Observation Network in the mouth areas of RFAZ. *Water Resour.* **49**, 796–807 (2022).
66. Hirsch, R. M. & De Cicco, L. A. *User guide to Exploration and Graphics for RivEr Trends (EGRET) and DataRetrieval: R Packages for Hydrologic Data*. Report No. 4-A10, 104 (United States Geological Survey, 2015).
67. R Core Team *R: A Language and Environment for Statistical Computing* (R Foundation for Statistical Computing, 2022).
68. Lee, C. J. et al. An evaluation of methods for estimating decadal stream loads. *J. Hydrol.* **542**, 185–203 (2016).
69. Hirsch, R. M. Large biases in regression-based constituent flux estimates: causes and diagnostic tools. *JAWRA J. Am. Water Resour. Assoc.* **50**, 1401–1424 (2014).
70. Zhang, Q. & Hirsch, R. M. River water-quality concentration and flux estimation can be improved by accounting for serial correlation through an autoregressive model. *Water Resour. Res.* **55**, 9705–9723 (2019).
71. Pohlert, T. trend: Non-parametric Trend Tests and Change-Point Detection. R version 1.1.4 https://CRAN.R-project.org/package=trend (2020).
72. Hirsch, R. M., Slack, J. R. & Smith, R. A. Techniques of trend analysis for monthly water quality data. *Water Resour. Res.* **18**, 107–121 (1982).
73. Hirsch, R. M. & Slack, J. R. A nonparametric trend test for seasonal data with serial dependence. *Water Resour. Res.* **20**, 727–732 (1984).
74. McClelland, J. W. et al. Particulate organic carbon and nitrogen export from major Arctic rivers. *Glob. Biogeochem. Cycles* **30**, 629–643 (2016).
75. Wickham, H. *ggplot2: Elegant Graphics for Data Analysis* (Springer-Verlag, 2016).
76. Warnes, G. R. et al. gplots: Various R Programming Tools for Plotting Data. R version 3.1.3 https://CRAN.R-project.org/package=gplots (2022).
77. *The Resources of Surface Waters of the USSR. Hydrological Knowledge* Vols. 15, 16, 17, 19 (Gidrometeoizdat, 1965–1969).

78. Holmes, R. M. et al. in *Climatic Change and Global Warming of Inland Waters: Impacts and Mitigation for Ecosystems and Societies* (eds Goldman, C. R. et al.) (Wiley, 2013).
79. Rodell, M. et al. The global land data assimilation system. *Bull. Am. Meteorol. Soc.* **85**, 381–394 (2004).
80. Lehner, B. et al. High-resolution mapping of the world's reservoirs and dams for sustainable river-flow management. *Front. Ecol. Environ.* **9**, 494–502 (2011).
81. Gelaro, R. et al. The modern-era retrospective analysis for research and applications, version 2 (MERRA-2). *J. Clim.* **30**, 5419–5454 (2017).
82. Center for International Earth Science Information Network–CIESIN–Columbia University. Gridded Population of the World, version 4 (GPWv4): population density, revision 11. *NASA Socioeconomic Data and Applications Center* https://doi.org/10.7927/H49C6VHW (2018).
83. Lammers, R. B., Shiklomanov, A. I., Vorosmarty, C. J., Fekete, B. M. & Peterson, B. J. Assessment of contemporary Arctic river runoff based on observational discharge records. *J. Geophys. Res. Atmos.* **106**, 3321–3334 (2001).

Acknowledgements

Funding for the PARTNERS programme and Arctic Great Rivers Observatory has been provided via US National Science Foundation grants 0229302 and 0732985 (B.J.P.); 0732522, 1107774, 1602615 and 1913888 (R.M.H.); 0732821, 1602680, 1914215 and 2230812 (J.W.M.); 0732583 (P.A.R.); 1603149 and 1914081 (R.G.M.S.); and 1602879 and 1913962 (A.I.S.). This work would not have been possible without contributions from many individuals at the six ArcticGRO sampling locations, and we gratefully acknowledge contributions from E. Amos, B. Blais, C. Couvillion, A. Davydova, N. Dion, V. Efremov, L. Kutny, R. McLeod, R. Myers, A. Pavlov, A. Smirnov, M. Suslov, G. Zimova and support from the Environment and Climate Change Canada and Indigenous and Northern Affairs Canada offices in Inuvik, Canada. Sample collection occurred within the Gwich'in Settlement Region (Mackenzie River at Tsiigehtchic) and on the traditional territories of the Yup'ik people (Yukon River at Pilot Station) in North America and the Nenets, Dolgans, Nganasans, Evenks and Chukchi people (Ob', Yenisey, Lena and Kolyma rivers at Salekhard, Dudinka, Zhigansk and Chersky) in Russia. S. Sylva, G. Swarr and M. Auro assisted with analyses of major and trace anion/cation data.

Author contributions

Conceived of the paper and performed data analysis: S.E.T., R.M.H., J.W.M., R.G.M.S., A.S., F.M. and A.I.S. Led manuscript preparation: S.E.T. Initial design of the ArcticGRO (PARTNERS) programme: B.J.P., R.M.H., J.W.M., P.A.R., R.G.S., R.M.W.A., L.W.C., V.V.G., S.Z. and A.V.Z. Sample and data acquisition: A.V.Z., T.Yu.G., S.Z., N.Z., G.E., P.F.S., E.A.M., R.S., M.T. and L.S.K. Performed laboratory analyses: A.S., L.S., B.P.-E., C.G. and P.F.S. Read and commented on the manuscript: all authors.

Competing interests

The authors declare no competing interests.

Additional information

Extended data is available for this paper at https://doi.org/10.1038/s41561-023-01247-7.

Supplementary information The online version contains supplementary material available at https://doi.org/10.1038/s41561-023-01247-7.

Correspondence and requests for materials should be addressed to Suzanne E. Tank.

Peer review information *Nature Geoscience* thanks Fabrice Lacroix, Ryan Toohey and the other, anonymous, reviewer(s) for their contribution to the peer review of this work. Primary Handling Editor: Xujia Jiang, in collaboration with the *Nature Geoscience* team.

https://doi.org/10.1038/s41561-023-01247-7

Extended Data Table 1 | Characteristics of the six largest Arctic watersheds

	Watershed Area	Area at gauge	Distance to Arctic Ocean[a]	Mean discharge[b] (2003-2019)	Runoff (2003-2019)	Permafrost[c]	Continuous Permafrost[c]	Discontinuous Permafrost[c]	Tundra[d]	Forest[d]	Regulated[e]	Mean annual temperature (2003-2019)[f]	Mean annual precipitation (2003-2019)[f]	Population Density[g]
	10^6 km^2	10^6 km^2	km	km^3 y^{-1}	mm y^{-1}	(% area)	(% area)	(% area)	(% area)	(% area)	(% area)	°C	mm y^{-1}	people km^{-2}
Ob'	2.99	2.95	287	409	139	26	2	4	0.1	48.2	14.6	-0.7	604	9.07
Yenisey	2.54	2.44	433 (697)	595	244	88	33	11	0.5	67.9	50.5	-4.4	619	2.85
Lena	2.46	2.43	754 (211)	599	247	99	79	11	1.2	62.5	7.2	-8.9	548	0.45
Kolyma	0.65	0.53	120 (283)	108	205	100	100	0	3.2	16.7	18.9	-10.7	546	0.2
Yukon	0.83	0.83	200	211	254	99	23	66	0.1	68.4	0.0	-4.8	571	0.17
Mackenzie	1.78	1.68	260	295	176	82	16	29	0.0	74.2	4.3	-3.6	547	0.25
Sum	11.25	–		2,217	–	–	–	–	–	–	–	–	–	–
Pan-Arctic[h]	16.8	–	–	~3710[i]	~220	–	–	–	–	–	–	–	–	–

[a]Distance from the water chemistry station (discharge gauge) to the Arctic Ocean, including transit distance through river mouth deltas. Where only one value is presented, water chemistry and discharge data collection are co-located. Data for Russian rivers are from the Hydrometeorological Service of the USSR[77]. Data for North American rivers are estimated from Google Earth. [b]Mean annual discharge over the study period. [c]From Holmes et al. (2013)[78]. Permafrost extent and classification from the International Permafrost Association's Circum-Arctic Map of Permafrost and Ground Ice Conditions. [d]Vegetation classes from the 20-class GLDAS/NOAH product[79], based on a 30 arc second MODIS vegetation data that uses a modified IGBP classification scheme. Tundra is the sum of mixed and bare ground tundra. Forest is the sum of evergreen, deciduous, and mixed forest, and wooded tundra. [e]Regulated area at the end of the study period, from Lehner et al. (2011)[80]. Includes impoundments that were completed on the Kolyma (2013) and Yenisey (2012) rivers. [f]Mean annual temperature and precipitation from the MERRA2 reanalysis product[81]. [g]Population density from the Center for International Earth Science Information Network (2018)[82] gridded population of the world. [h]Watershed area of 16.8 x 10^6 km^2 corresponds to the area demarcated in Figure 1, which does not include drainage to Hudson Bay. The pan-Arctic watershed including Hudson Bay, but excluding the Greenland Ice Cap, covers an area of 22.4 x 10^6 km^2 (from Lammers et al. [2001][83]). [i]Estimate derived from Shiklomanov et al. (2021)[24], for the period covering 1980-2018.

https://doi.org/10.1038/s41561-023-01247-7

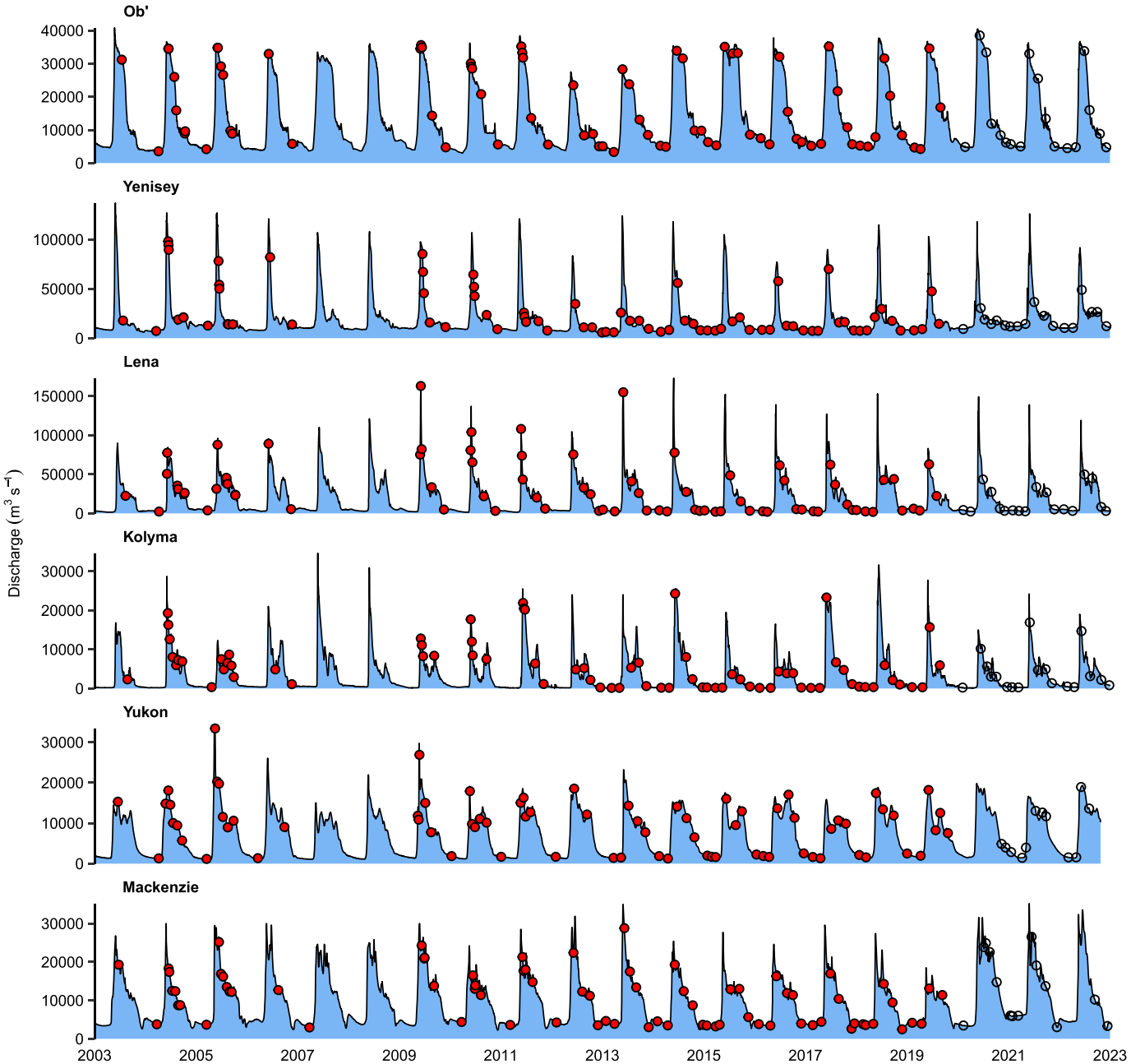

Extended Data Fig. 1 | Time-series of discharge and concentration measurements across the six great Arctic rivers. Discharge is shown as a continuous record for all rivers. Dates of sample collection for concentration measurements used in this analysis are shown with red circles; hollow circles indicate ongoing data collection.

https://doi.org/10.1038/s41561-023-01247-7

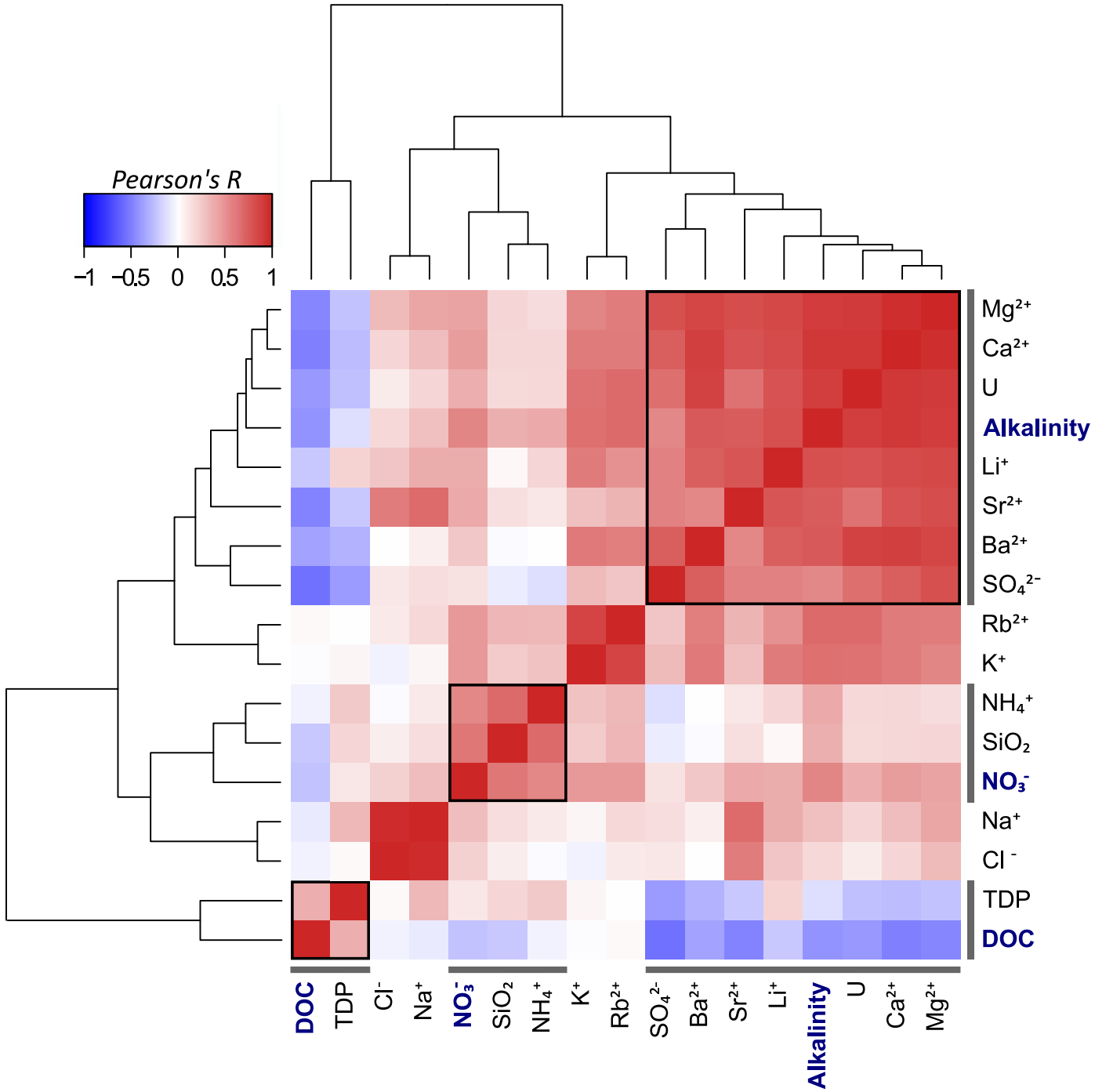

Extended Data Fig. 2 | Correlation between constituents for the full ArcticGRO dataset. Shading indicates the Pearson correlation coefficient, which was used as the distance metric for hierarchical clustering. Focal constituents (alkalinity, nitrate [NO_3^--N], and dissolved organic carbon [DOC]) are bolded in blue. Black boxes within the correlation plot and grey shading along axes indicate clusters associated with each focal constituent. Analysis is visualized via a cluster heatmap, for correlations on individual concentration data points.

https://doi.org/10.1038/s41561-023-01247-7

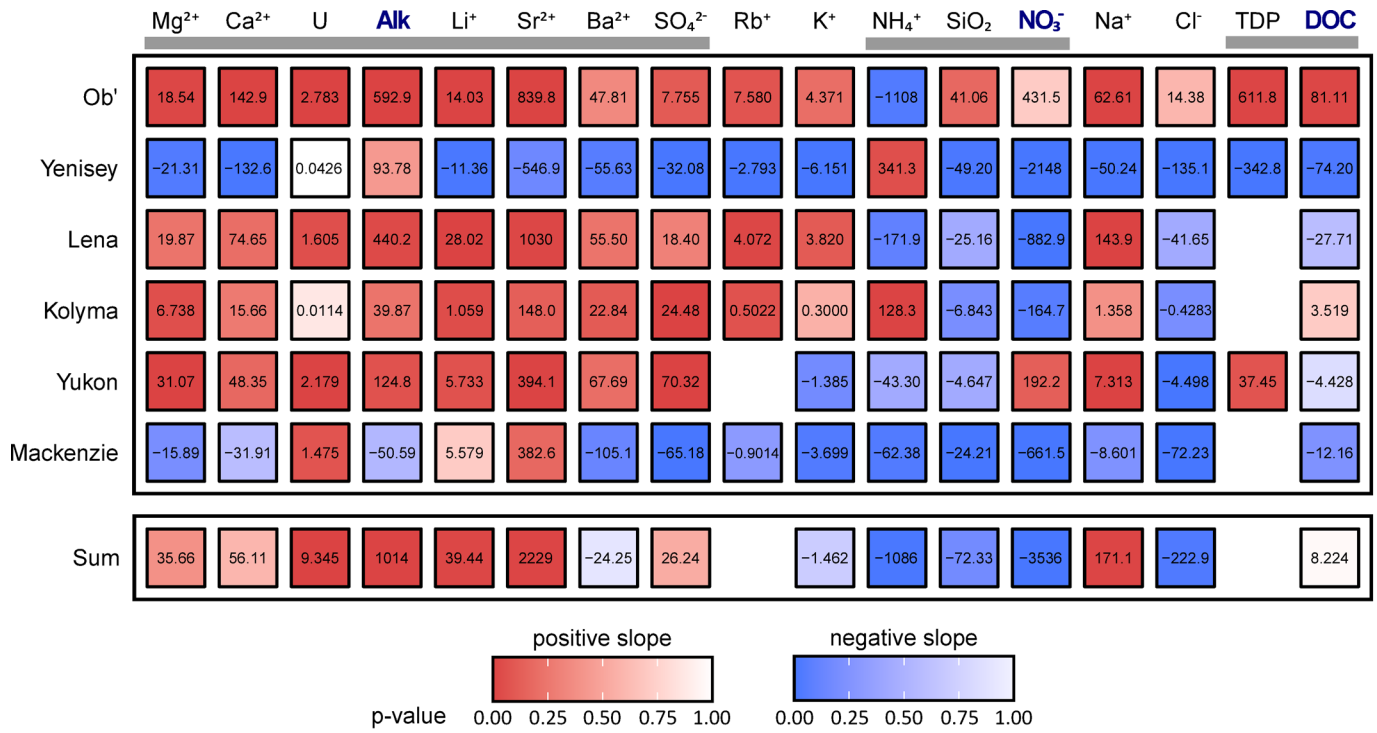

Extended Data Fig. 3 | Annual trends in constituent flux across the full ArcticGRO dataset. Trend analysis is via a Mann-Kendall analysis; the Thiel-Sen slope (numerical value) and p-value of the trend analysis (shading) are shown. Corresponding trends in concentration are provided in Extended Data Fig. 4. Grey bars illustrate groupings from Extended Data Fig. 2. Units (Gg y^{-1} or Mg y^{-1}) are provided in Supplementary Table 1.

https://doi.org/10.1038/s41561-023-01247-7

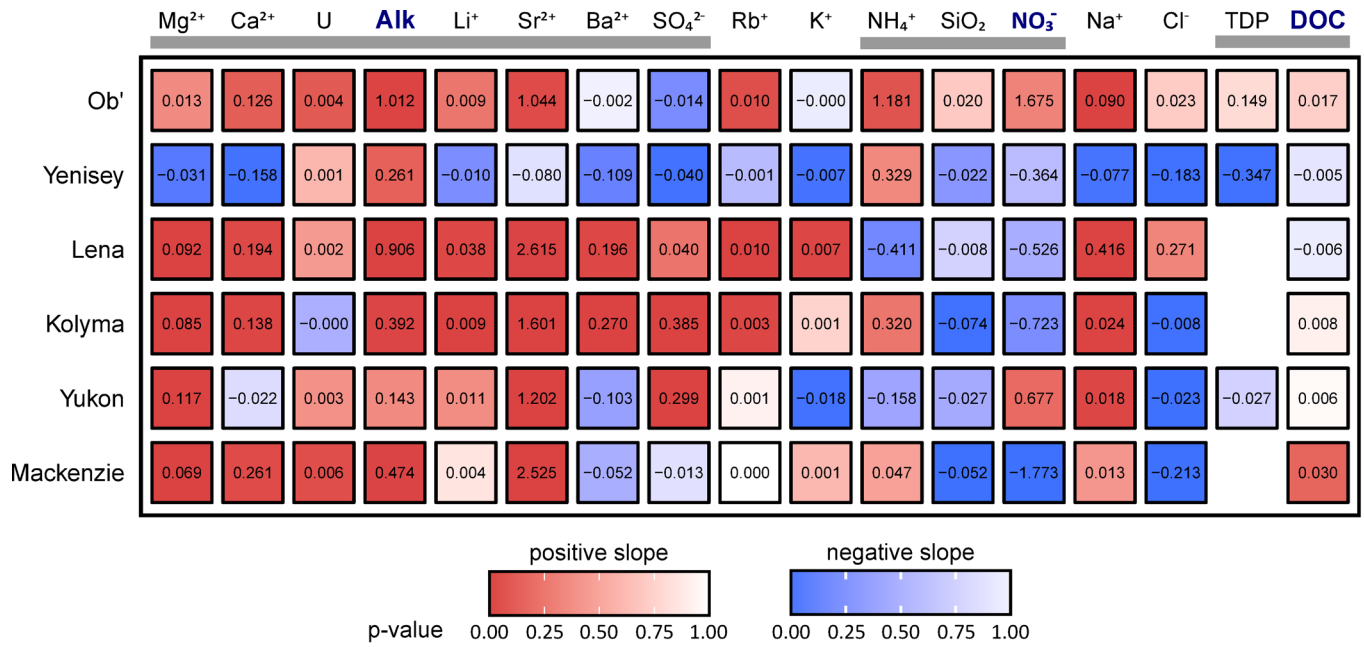

Extended Data Fig. 4 | Trends for constituent concentration across the full ArcticGRO dataset. Trend analysis is via a seasonal Mann-Kendall analysis; the Thiel-Sen slope (numerical value) and p-value of the trend analysis (shading) are shown. Corresponding trends in constituent flux are provided in Extended Data Fig. 3. Grey bars illustrate groupings from Extended Data Fig. 2. Units (mg L^{-1} y^{-1} or µg L^{-1} y^{-1}) are provided in Supplementary Table 2.

https://doi.org/10.1038/s41561-023-01247-7

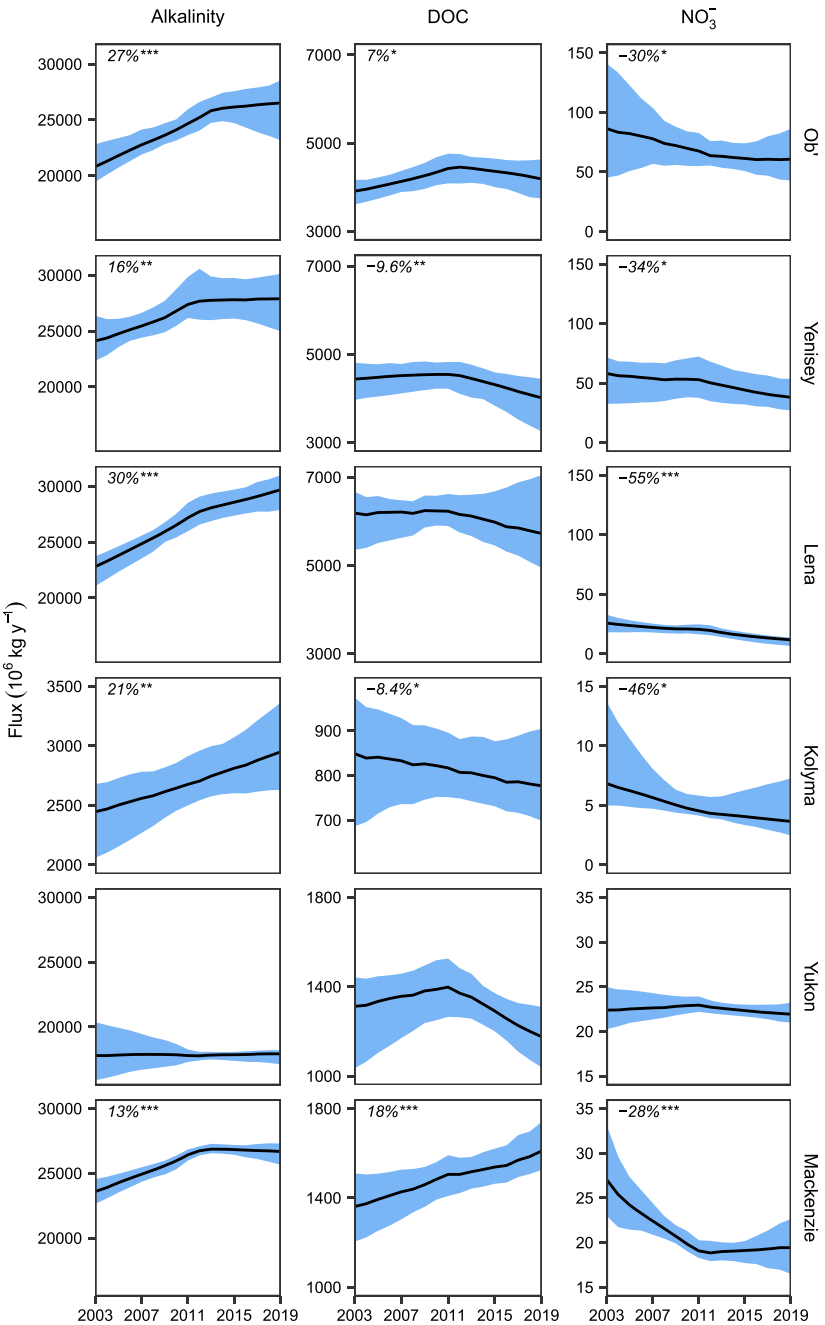

Extended Data Fig. 5 | Flow-normalized trends in annual constituent flux. Trends are provided for the three focal constituents (alkalinity, dissolved organic carbon [DOC], and nitrate [NO_3^--N], for each of the six great Arctic rivers. The solid line indicates the mean, and shading indicates 90% confidence interval from the block bootstrap analysis. Asterisks indicate block bootstrap-assessed trends that are: ***highly likely (posterior mean estimate $\hat{\pi}$ <0.05 or >0.95); **very likely ($\hat{\pi}$ 0.05–0.10 or 0.90–0.95); or *likely ($\hat{\pi}$ 0.10–0.33 or 0.66–0.90), with percentage change in constituent flux indicated for the period of record. Where no percentage change is shown, trends were assessed to be about as likely as not ($\hat{\pi}$ 0.33–0.66).